Supporting Information

Efficient catalytic conversion of CO$_2$ to quinazoline-2,4(1*H*,3*H*)-diones by dual-site anion-functionalized ionic liquid: reconsidering the mechanism

Tingting Chen, Yujun Guo and Yingjie Xu*

Department of Chemistry, Shaoxing University, Shaoxing, Zhejiang Province, 312000, China.

Email: xuyj@usx.edu.cn

1. Experimental section: preparation of $[P_{4442}]_2[Hy]$ and quinazoline-2,4(1*H*,3*H*)-diones

1.1 Materials

Tributylphosphine (P_{444}, >95%), bromoethane (C_2H_5Br, >99%), sodium hydroxide (NaOH, >99%), hydantoin (Hy, >99%), acetonitrile (CH_3CN, >98%), ethanol (>99%) 2-aminobenzonitrile ($C_7H_6N_2$, >99%), potassium hydrogen phthalate ($C_8H_5O_4K$, 99.99%), and a basic anion-exchange resin (Amberlite 717, AR) were purchased from Aladdin Reagent Co. Ltd., Shanghai, China. Trichloromethane ($CHCl_3$, >99%) was purchased from Tokyo Chemical Industry Co., Ltd. CO_2 (>99.9%) and N_2 (>99.999%) were purchased from Shaoxing Zhongxu Gas Factory. All chemicals were used as received and obtained in highest purity grade possible.

## 1.2 Synthesis and characterization of $[P_{4442}]_2[Hy]$
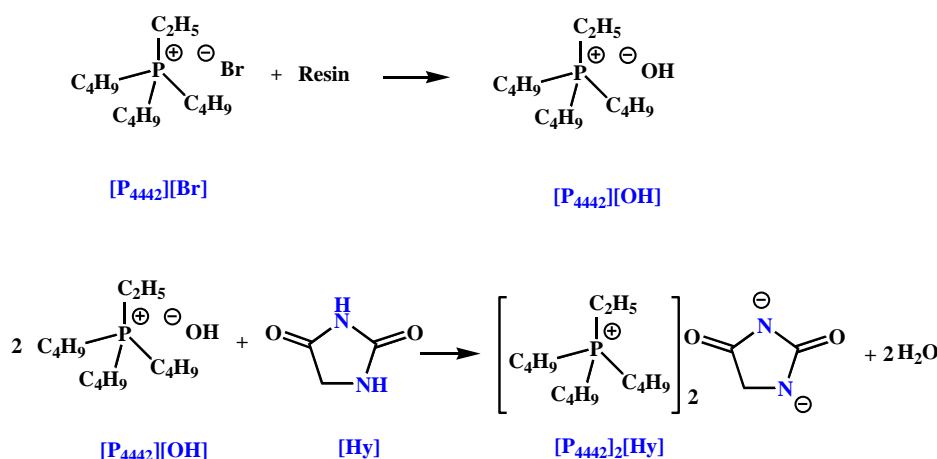
Scheme S1. Synthesis of $[P_{4442}]_2[Hy]$

The synthesis process of $[P_{4442}]_2[Hy]$ is similar to the literature.[1] Firstly, P_{444} and C_2H_5Br were reacted under N_2 protection to give the tributylethylphosphonium bromide ($[P_{4442}]Br$). Secondly, $[P_{4442}]Br$ was passed through the basic anion-exchange resin activated by NaOH to give the tributylethylphosphonium hydroxide ($[P_{4442}][OH]$) ethanol solution, and its concentration was determined by titration of a potassium hydrogen phthalate solution. Finally, $[P_{4442}]_2[Hy]$ was synthesized by neutralization of $[P_{4442}][OH]$ with Hy in a 2:1 molar ratio at room temperature for 48 h. The specific reaction equations are shown in Scheme S1. A large amount of ethanol and a small amount of water were removed from the $[P_{4442}]_2[Hy]$ under vacuum at 343.15 K. Tace amounts of water were removed from $[P_{4442}]_2[Hy]$ by a freeze dryer. The water content in $[P_{4442}]_2[Hy]$ determined by Karl Fisher titration (Mettler Toledo C20S) was 1000 ppm. The structure of $[P_{4442}]_2[Hy]$ was characterized by ^1H NMR and ^{13}C NMR spectra with Bruker AVANCE III 400MHz spectrometer (Fig. S1). The thermal stability of $[P_{4442}]_2[Hy]$ was obtained

by measuring its thermogravimetric analysis (TGA) curves under N_2 of 60 mL/min at 10 °C/min (Fig. S2).

1.3 Typical process for the [P$_{4442}$]$_2$[Hy] catalyzed conversion of CO$_2$ to quinazoline-2,4(1H,3H)-diones and reusability of [P$_{4442}$]$_2$[Hy]
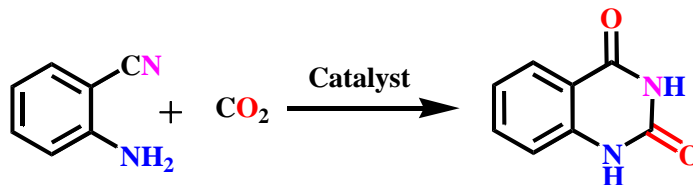
Scheme S2. [P$_{4442}$]$_2$[Hy] catalyzed conversion of CO_2 to quinazoline-2,4(1H,3H)-diones.

2-Aminobenzonitrile (4 mmol) and [P$_{4442}$]$_2$[Hy] (0.8 mmol) were added to a round bottom flask containing a magnet, CO_2 was passed through to blow out the air in the flask, a CO_2 balloon was connected to the flask, the CO_2 pressure was ensured to be 0.1 MPa and stirred at 353.15 K for 24 h, the reaction equations were shown in Scheme S2. The progress of the reaction was monitored by HPLC (Zorbax RX-C8 column, the mobile phase was acetonitrile: water = 5:5 in volume ratio, the detection wavelength λ was 245 nm) and the content of quinazoline-2,4(1H,3H)-diones was determined by the external standard method in order to calculate the product yield (Fig. S3). The effect of the amount of [P$_{4442}$]$_2$[Hy], temperature, time, and CO_2 pressure on the reaction were studied, the obtained results were shown in Fig. S4.

After the reaction, the system was layered by adding 10 mL distilled water and stirring, the upper layer consisting [P$_{4442}$]$_2$[Hy] and water, the lower layer being the product. The product was obtained by centrifugation and washed three times with distilled water and ether, respectively. The product was dried under vacuum at 338.15 K for 12 h to obtain a white powder (quinazoline-2,4(1H,3H)-diones), the structure of product was characterized by NMR (Fig. S5) and the isolated yield were calculated. In addition, the water in the upper [P$_{4442}$]$_2$[Hy] + water mixture was removed to obtain [P$_{4442}$]$_2$[Hy], which was dried in freeze dryer for 24 h to remove trace water, and then the recovered [P$_{4442}$]$_2$[Hy] was used for the next catalytic reaction (Fig. S6).

2. The thermodynamics and kinetics of the reaction

Van't Hoff equation was shown in Eq. S1. Where K was the equilibrium constants and could be calculated from Fig. S4a. The relationship betwwen K and $1/T$ was plotted in Fig. S7. The kinetic equation for the catalytic conversion of CO_2 and 2-aminobenzonitrile to quinazoline-2,4(1H,3H)-diones by [P$_{4442}$]$_2$[Hy] was developed and was shown in Eq. S2. Since CO_2 is in excess under the optimal reaction conditions and the catalyst [P$_{4442}$]$_2$[Hy] is used in a constant amount, the kinetic equation can be simplified to Eq. S3, where k (h^{-1}) and k' (h^{-1}) are the

reaction rate constant.[2, 3] Assuming that the reaction is a first-order reaction, Eq. S3 simplifies to the differential (Eq. S4) and integral (Eq. S5) equations for the first-order reaction kinetics. Where C_A represents the concentration of reactants during the reaction and C_0 represents the initial reactant concentration. Eq. S6 and Eq. S7 are the Arrhenius equations, and the relationship betwwen k' and $1/T$ was plotted in Fig. S8.

$$\ln K = -\Delta H/RT + \Delta S/R \qquad \textbf{Eq. S1}$$

$$\text{Rate} = dx/dt = k\,(\text{2-aminobenzonitrile})^a(CO_2)^b([P_{4442}]_2[Hy])^c \qquad \textbf{Eq. S2}$$

$$\text{Rate} = dx/dt = k'\,(\text{2-aminobenzonitrile})^a \qquad \textbf{Eq. S3}$$

$$\text{Rate} = dx/dt = k'\,(\text{2-aminobenzonitrile})^1 \qquad \textbf{Eq. S4}$$

$$-\ln[C_A/C_0] = k'\,t \qquad \textbf{Eq. S5}$$

$$k' = A\exp(-E_a/RT) \qquad \textbf{Eq. S6}$$

$$\ln k' = \ln A - E_a/RT \qquad \textbf{Eq. S7}$$

3. Computation method

The DFT calculations were performed using the Gaussian 09 D.01 program,[4] with geometry optimizations at the B3LYP/6-31++G (d, p) basis set level for $[Hy]^{2-}$, CO_2, 2-aminobenzonitrile, possible intermediates formed by the reaction of the substrate with CO_2, and quinazoline-2,4(1H,3H)-diones, with the optimized geometry considered to be a local minimum with no imaginary frequencies. The Mulliken charges of $[Hy]^{2-}$, $[Hy]^-$, and $[1\text{-MHy}]^-$ were obtained using natural bond orbital (NBO) analysis (Fig. S9). The energies of the interactions between $[Hy]^{2-}$ and CO_2 (Fig. S10), and those between $[Hy]^{2-}$ and 2-aminobenzonitrile (Fig. S12), were calculated, where the enthalpy (ΔH) and Gibbs free energy (ΔG) was calculated as the difference between the energy of the complex and the sum of the energies of the optimized monomers. Moreover, the energies of the interactions during the conversion of substrates to intermediates and intermediates to products were calculated, where ΔH and ΔG of the conversion of substances was calculated as the difference between the energy of the complex and the sum of the energies of the optimized monomers.

4. Spectra experiment

^{15}N NMR spectra of of 2-aminobenzonitrile, $[P_{4442}]_2[Hy]$ and their mixtures (mole ratio = 1:1) were measured by Bruker AVANCE III 400MHz spectrometer. In order to eliminate the effect of

deuterated reagent-sample interaction on the N signal, the amount of DMSO-d_6 to sample was controlled to be a molar ratio of 1:1.

FT-IR spectra were recorded on a Nicolet 6700 Fourier transform infrared spectrometer equipped with a DTGS detector, KBr windows, and ATR accessory. Each ATR-IR spectrum was recorded with a resolution of 2 cm^{-1} and 16 parallel scans, and the wavenumber was in the range from 4000 to 600 cm^{-1}.[5,6] The reaction of CO_2 with 2-aminobenzonitrile catalyzed by [P$_{4442}$]$_2$[Hy] was carried out under optimal reaction conditions, and samples were taken from the reaction system at an interval of 4 hours for testing, and FT-IR spectra were obtained as shown in Fig. S11. FT-IR spectra of [P$_{4442}$]$_2$[Hy] before and after the absorption of CO_2 (ATR accessory) and quinazoline-2,4(1H,3H)-diones (KBr pressing method) were compared as shown in Fig. S13.

In situ FT-IR spectra were recorded using a ReactIR 702L (Mettler Toledo) equipped with a 9. 5 mm diameter DiComp ATR probe with a 1.5-meter fiber.[7,8] IR spectra were collected at 4 cm^{-1} resolution and 64 scans with a range of 3000−800 cm^{-1}. Diamond transmits IR over most of this region apart from absorption regions of 2200–1900 cm^{-1} and below 650 cm^{-1}.[9] This does not affect probe performance as the fingerprint region (1850–650 cm^{-1}) was used to monitor catalytic conversion of CO_2 and 2-aminobenzonitrile to quinazoline-2,4(1H,3H)-diones by [P$_{4442}$]$_2$[Hy]. The ATR probe equipped with RTO sensor was submerged in the reaction vessel, and spectra and temperature data collected throughout the reaction ([P$_{4442}$]$_2$[Hy]: 2-aminobenzonitrile as molar ratio 0.2:1 at a reaction temperature of 343.15 K with stirring and bubbling of 0.1 Mpa CO_2 with 60 mL/min). It should be noted that the background spectrum was collected at actual reaction conditions at the same data collection parameters and the same optical bench as subsequent reaction spectra, and was subtracted from the experimental data.
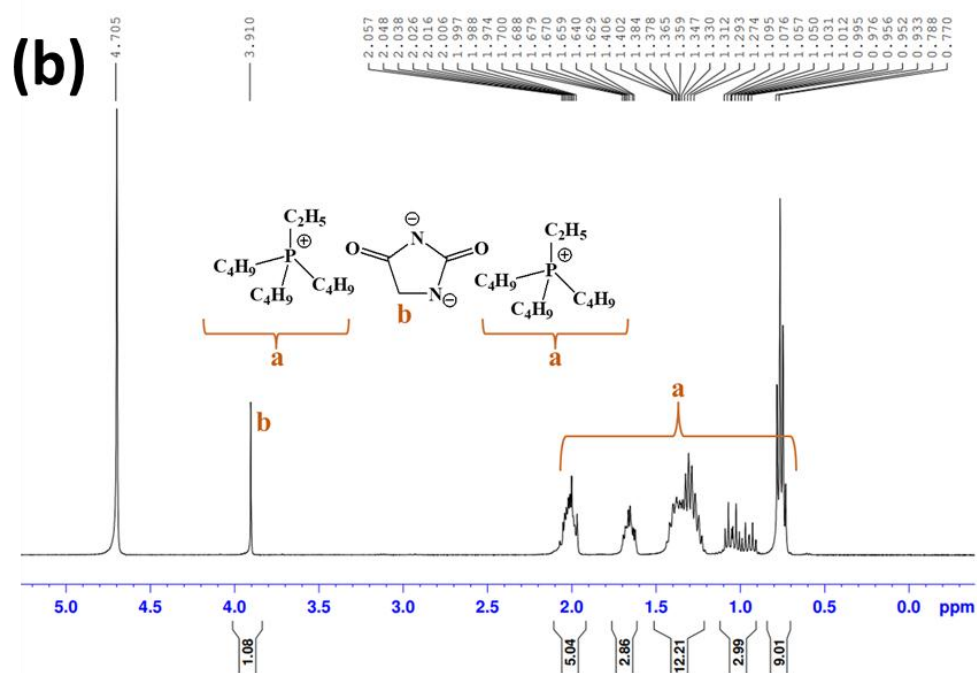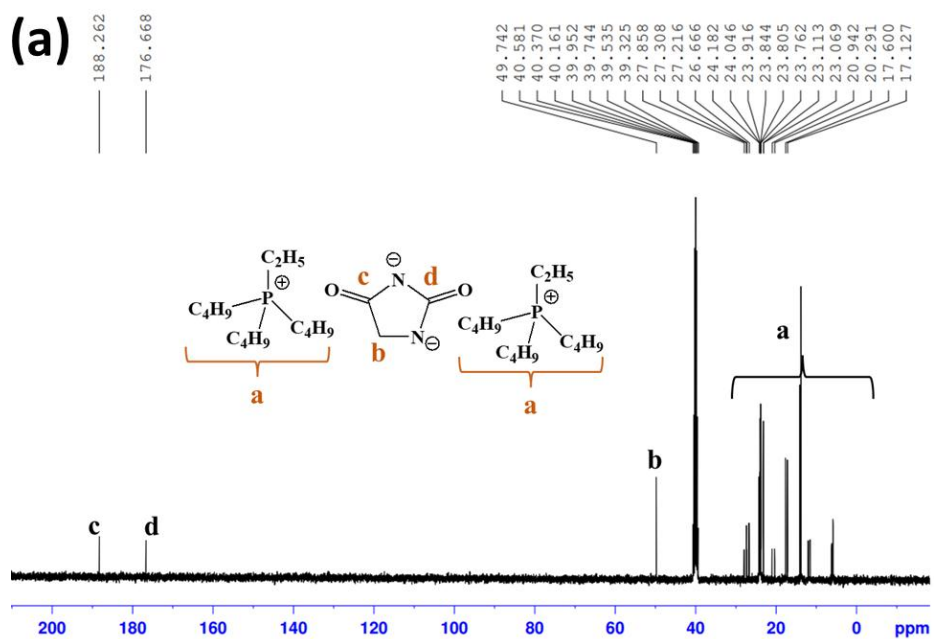
Fig. S1 (a) ^{13}C NMR (DMSO-d_6) of [P$_{4442}$]$_2$[Hy]: cation, 5.7-27.8 (CH$_3$, CH$_2$) ppm; anion, 49.7 (CH$_2$), 188.3, 176.7 (C=O) ppm; (b) ^{1}H NMR (D$_2$O) of [P$_{4442}$]$_2$[Hy]: cation, 0.77-0.96 (m, 9H, CH$_3$), 0.98-1.09 (m, 3H, CH$_3$), 1.27-1.41 (m, 12H, CH$_2$), 1.63-2.06 (m, 8H, PCH$_2$) ppm; anion, 3.91 (s, 2H, CH$_2$) ppm.
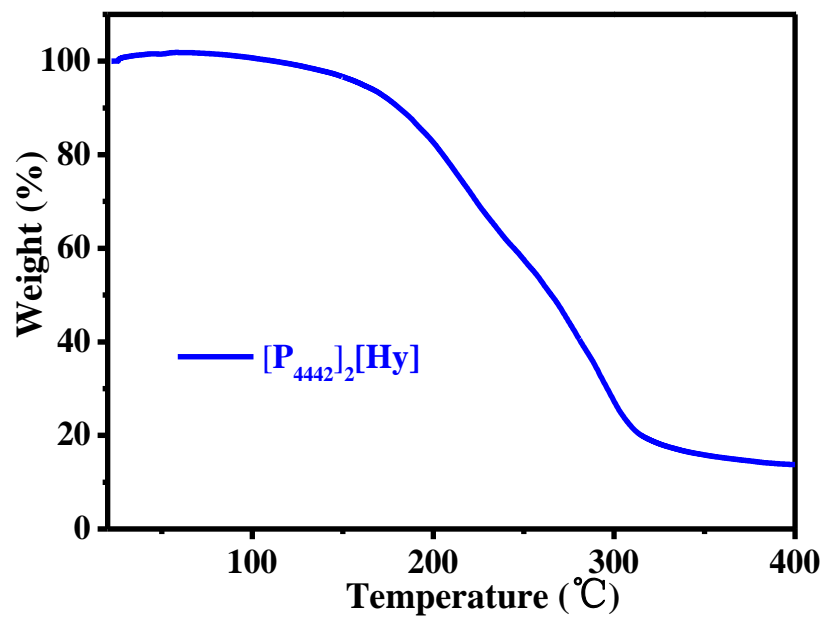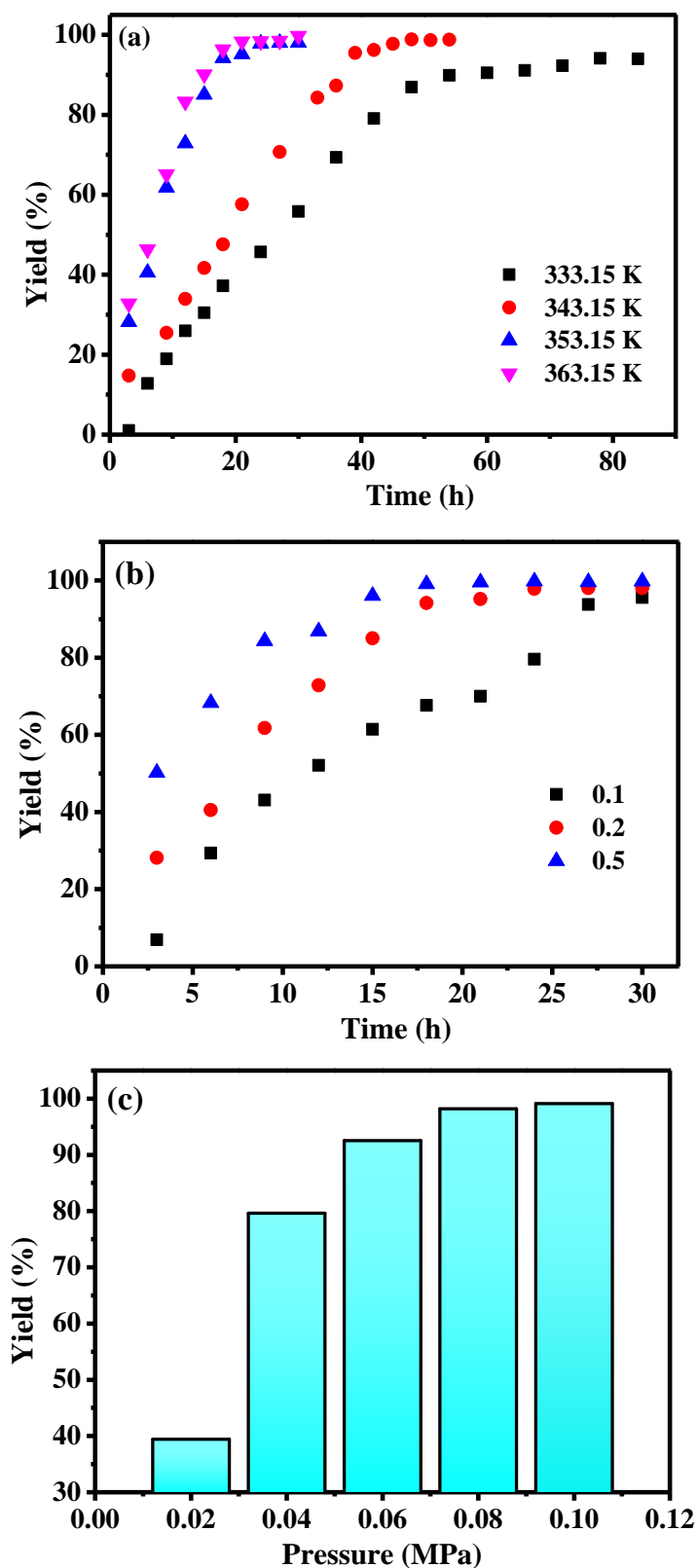
**Fig. S2** Thermogravimetric curve of [P$_{4442}$]$_2$[Hy].
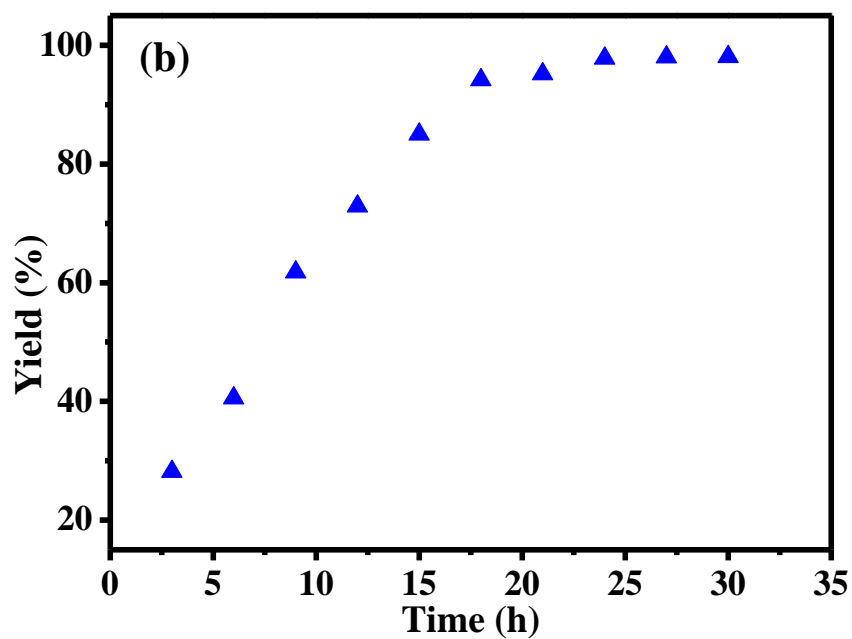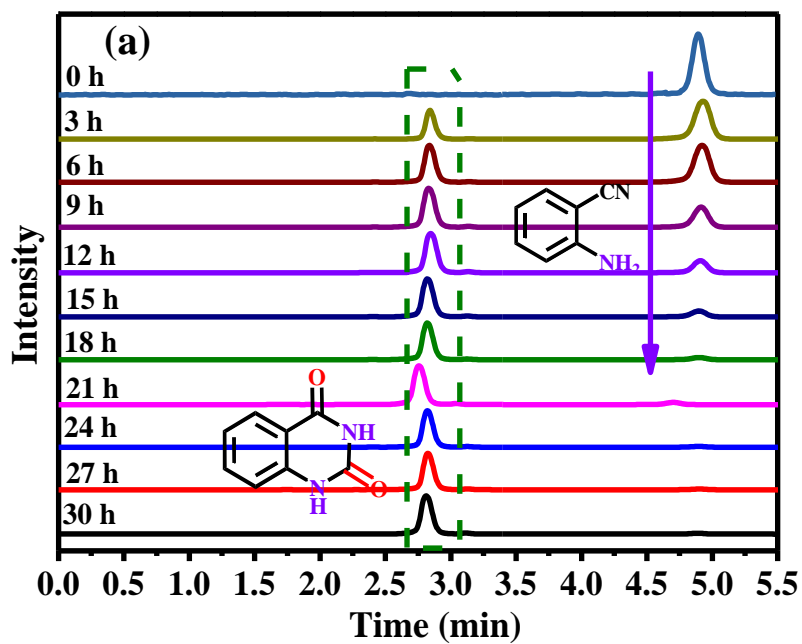
Fig. S3 The reaction of CO_2 with 2-aminobenzonitrile catalyzed by $[P_{4442}]_2[Hy]$ as a function of time at 0.1 Mpa CO_2 and 353.15 K, and the molar ratio of IL to 2-aminobenzonitrile of 0.2:1: (a) HPLC; (b) product yield.
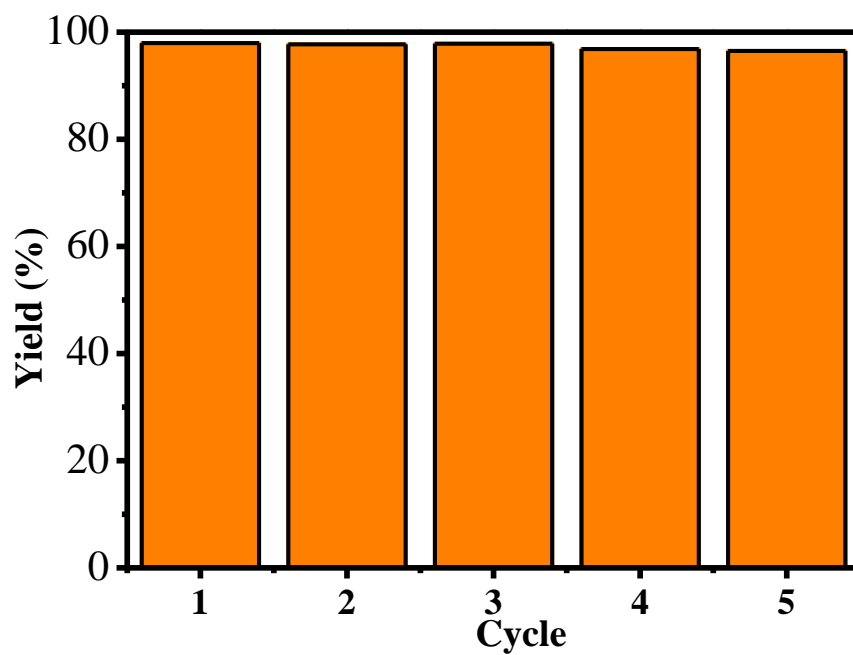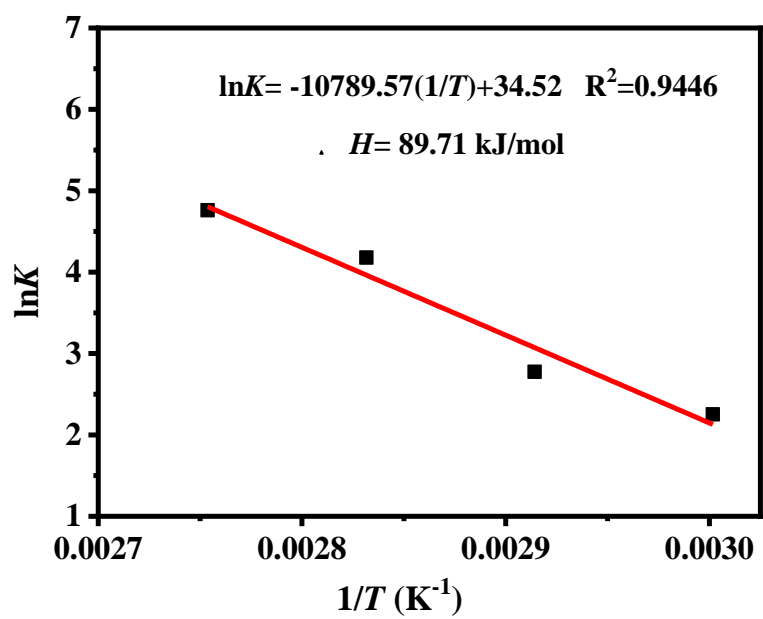
Fig. S4 The reaction of CO_2 with 2-aminobenzonitrile catalyzed by $[P_{4442}]_2[Hy]$: (a) the effect of the temperature at 0.1 Mpa CO_2 and the molar ratio of IL to 2-aminobenzonitrile of 0.2:1; (b) the effect of the amount of IL at 0.1 Mpa CO_2 and 353.15 K; (c) the effect of the CO_2 pressure at 353.15 K and the molar ratio of IL to 2-aminobenzonitrile of 0.2:1.
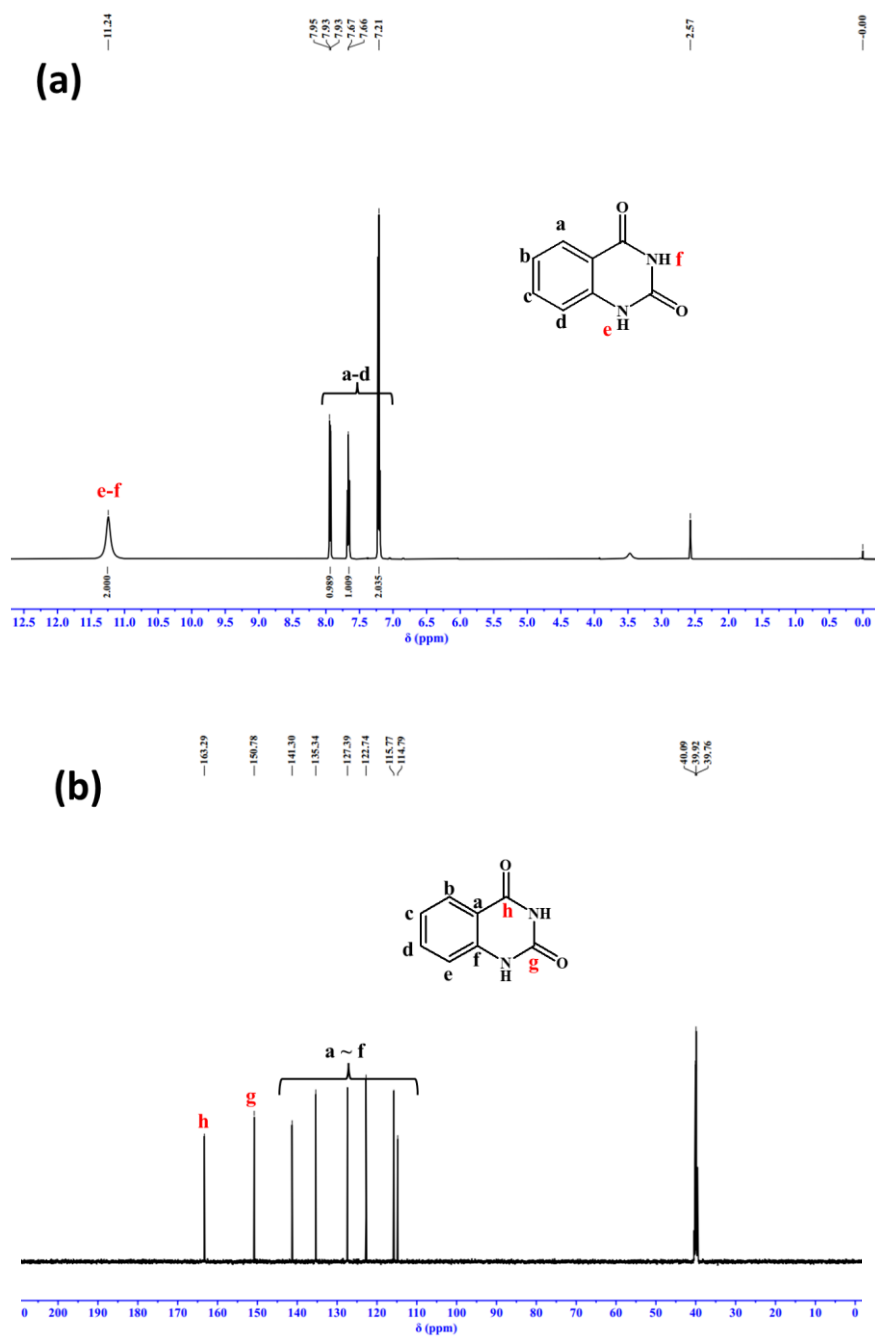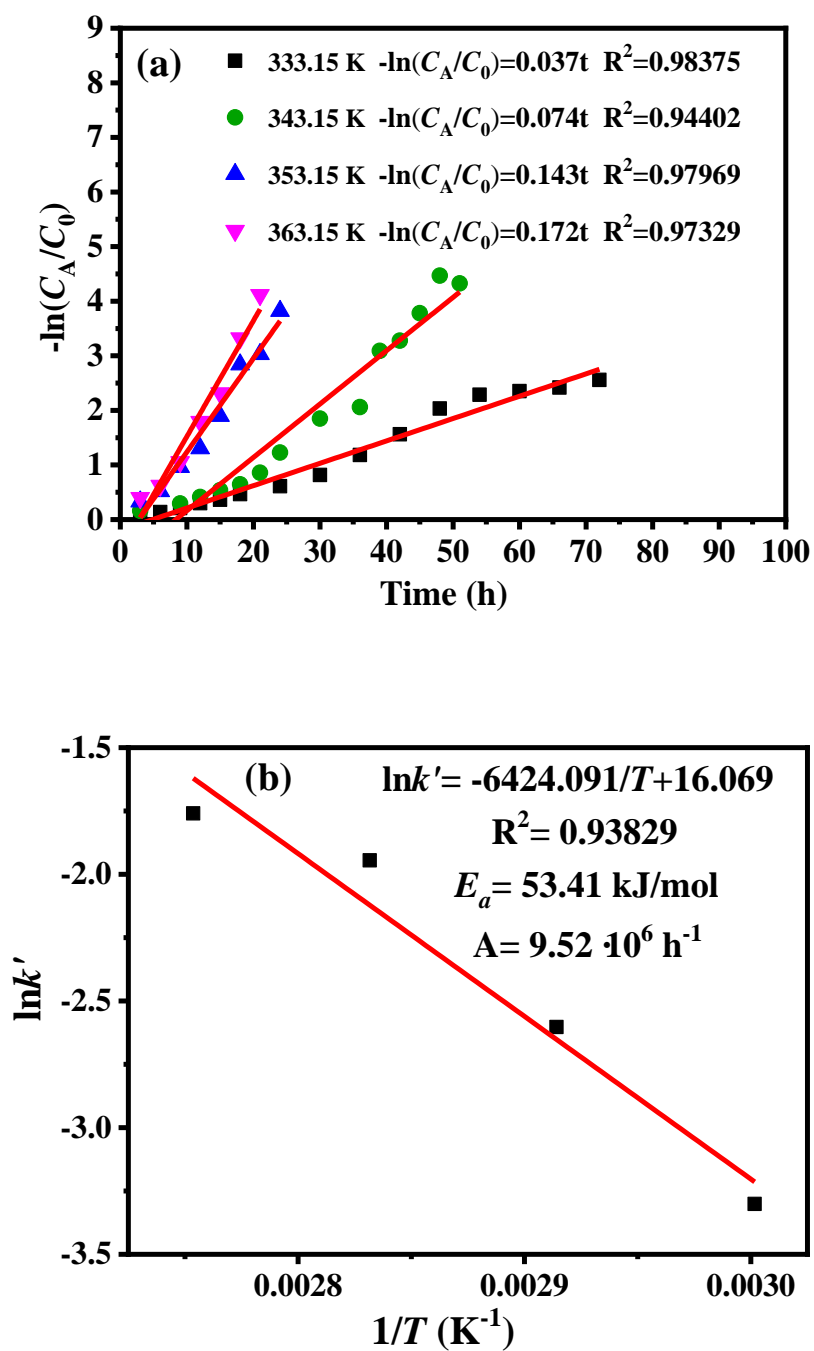
Fig. S5 (a) ^{1}H NMR (DMSO-d_6) of quinazoline-2,4(1H,3H)-diones: 7.2-8.0 (m, 4H, CH), 11.2 (s, 2H, NH) ppm; (b)^{13}C NMR (DMSO-d_6) of quinazoline-2,4(1H,3H)-diones: 114.8-141.3 (CH), 150.8, 163.3 (C=O) ppm.

Fig. S6 Reusability of [P$_{4442}$]$_2$[Hy] to catalyze CO$_2$ conversion for 5 cycles under optimal reaction conditions.

Fig. S7 The relationship between ln$K$ and $1/T$ of the reaction of CO_2 with 2-aminobenzonitrile catalyzed by [P$_{4442}$]$_2$[Hy].

(a)

■	333.15 K	$-\ln(C_A/C_0)=0.037t$ $R^2=0.98375$
●	343.15 K	$-\ln(C_A/C_0)=0.074t$ $R^2=0.94402$
▲	353.15 K	$-\ln(C_A/C_0)=0.143t$ $R^2=0.97969$
▼	363.15 K	$-\ln(C_A/C_0)=0.172t$ $R^2=0.97329$

(b)

$\ln k' = -6424.091/T + 16.069$

$R^2 = 0.93829$

$E_a = 53.41$ kJ/mol

$A = 9.52 \cdot 10^6$ h^{-1}

Fig. S8 The reaction of CO_2 and 2-aminobenzonitrile catalyzed by $[P_{4442}]_2[Hy]$ at different temperatures: (a) first-order reaction kinetics fitting curve; (b) fitted curve of Arrhenius equation.
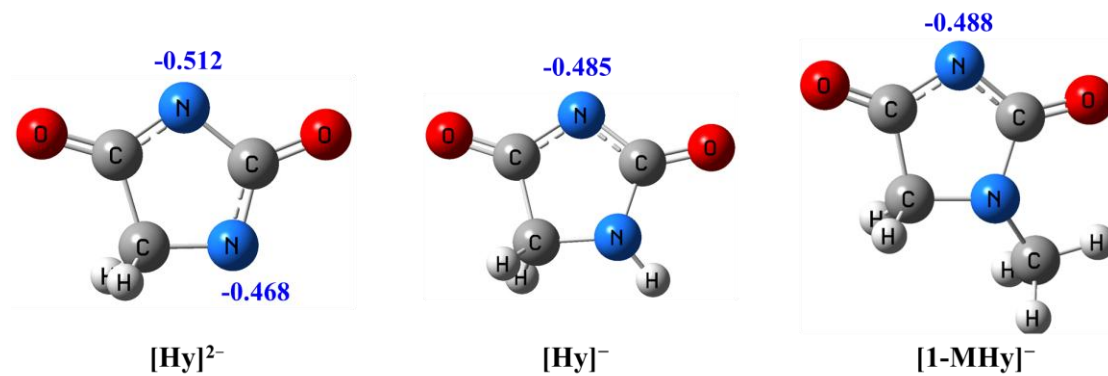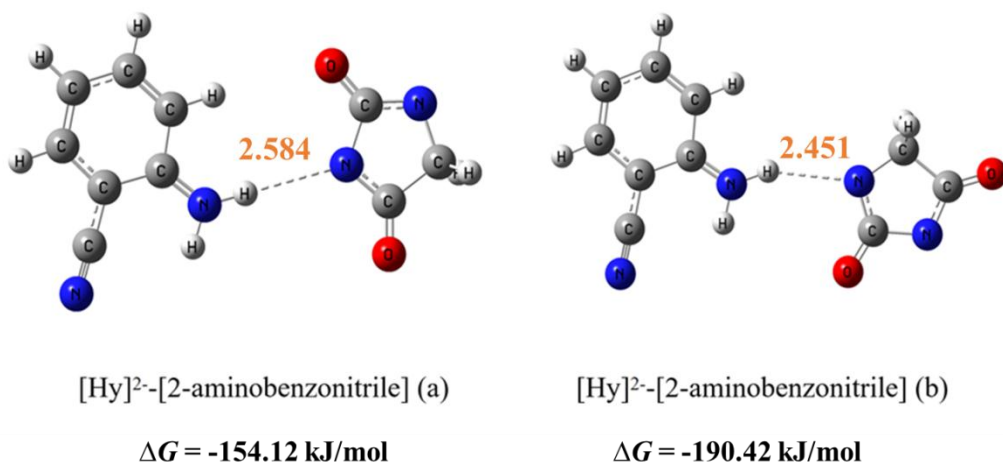
**Fig. S9** The optimized structure and Mulliken charges of three anions.

$\Delta G = \text{-106.35 kJ/mol}$ $\Delta G = \text{-164.60 kJ/mol}$ $\Delta G = \text{-168.94 kJ/mol}$
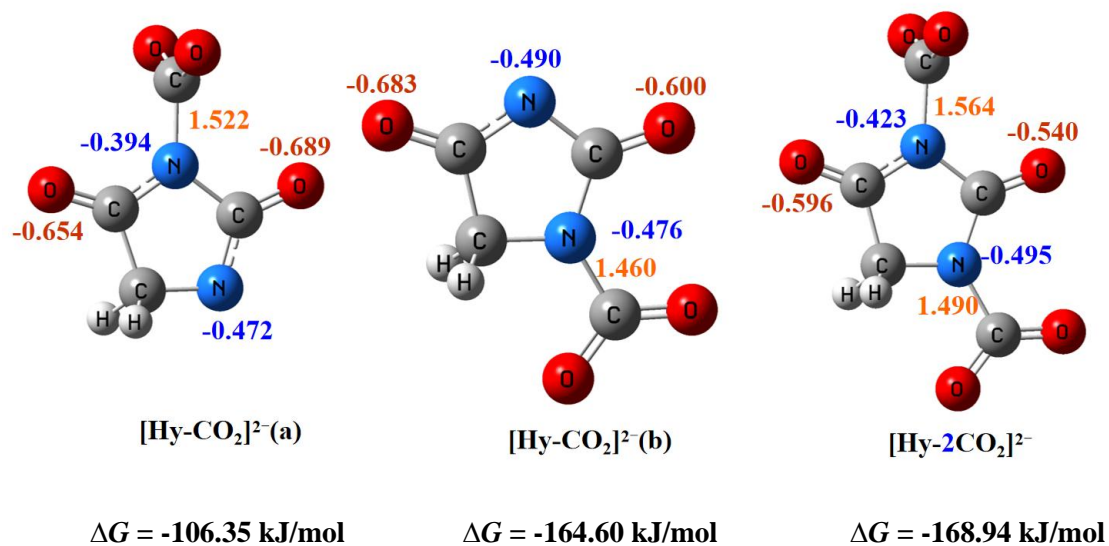
Fig. S10 The optimized structures and the calculated ΔG of $[\text{Hy-CO}_2]^{2-}$ and $[\text{Hy-2CO}_2]^{2-}$ intermediates.
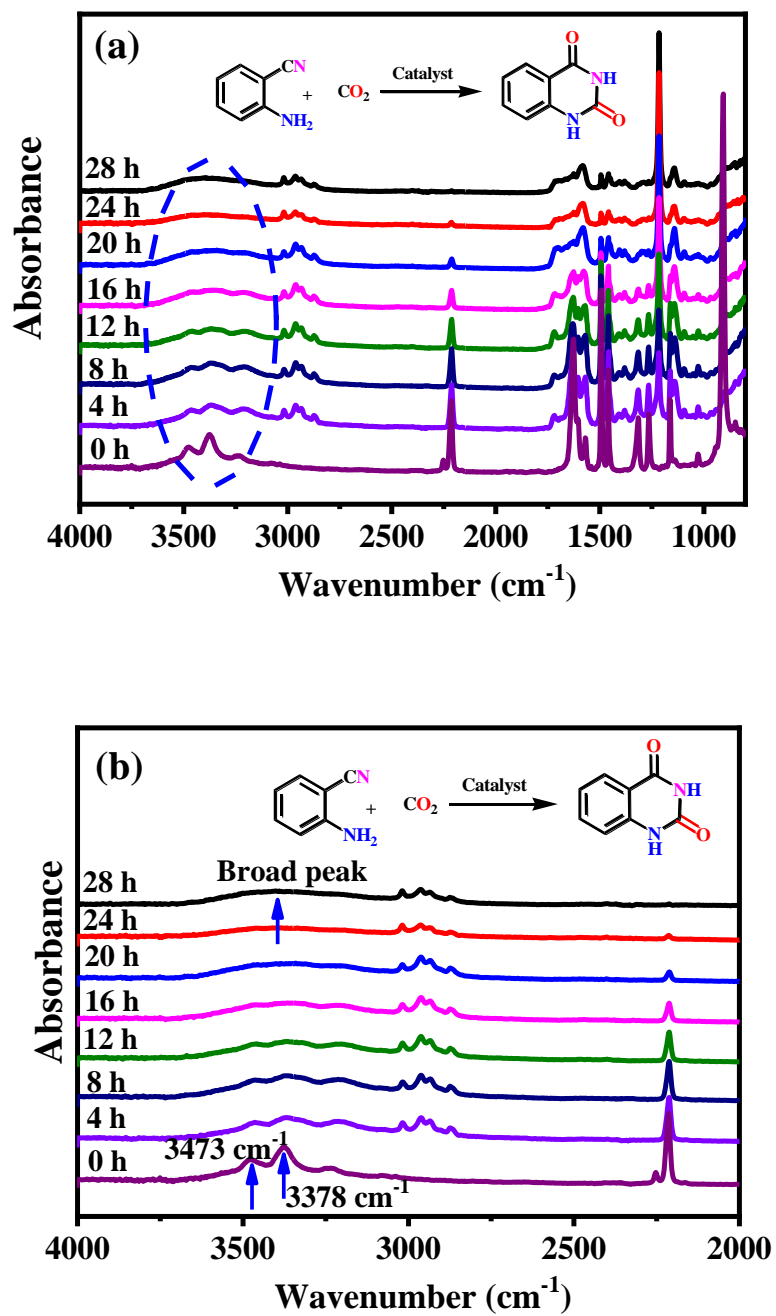
Fig. S11 FT-IR spectra of the reaction of CO_2 with 2-aminobenzonitrile catalyzed by [P_{4442}]$_2$[Hy] as a function of time: (a) 4000-800 cm^{-1}; (b) 4000-2000 cm^{-1}.

Fig. S12 The optimized hydrogen bonding between $[Hy]^{2-}$ and $-NH_2$ of 2-aminobenzonitrile.
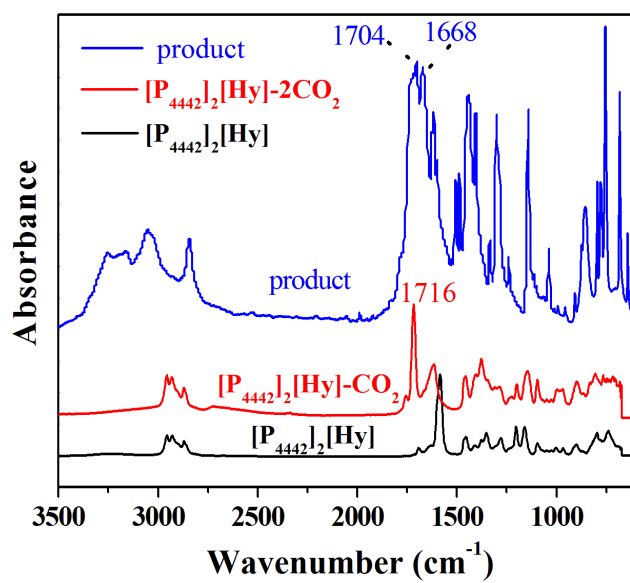
Fig. S13 FT-IR spectra of $[P_{4442}]_2[Hy]$ before and after the absorption of CO_2 (ATR accessory) and the isolated quinazoline-2,4(1H,3H)-diones (KBr pressing method)

References

1. (a) F. F. Chen, K. Huang, Y. Zhou, Z. Q. Tian, X. Zhu, D. J. Tao, D. E. Jiang and S. Dai, *Angew. Chem.*, *Int. Ed.*, 2016, **55**, 7166-7286; (b) C. Wang, X. Luo, H. Luo, D. E. Jiang, H. Li and S. Dai, *Angew. Chem.*, *Int. Ed.*, 2011, **50**, 4918-4922.

2. R. Luo, X. Zhou, Y. Fang and H. Ji, *Carbon*, 2015, **82**, 1-11.

3.B. Sarmah and R. Srivastava, *Ind. Eng. Chem. Res.*, 2017, **56**, 8202-8215.

4. M. Frisch and F. Clemente, *Wallingford, CT*, 2009, 20-44.

5. Y. Xu, T. Li, C. Peng and H. Liu, *Ind. Eng. Chem. Res.*, 2015, **54**, 9038-9045.

6. J. Liu, X. Tang, H. Lu and Y. Xu, *ACS Sustainable Chem. Eng.*, 2021, **9**, 5050-5060.

7. L. Wang, F. Zhang, Y. Liu, S. Du and J. Leng, *ACS Appl. Mater. Interfaces*, 2021, **13**, 18110-18119.

8. A. Castro-Ruiz, L. Grefe, E. Mejía and S. G. Suman, *Dalton T.*, 2023, **52**, 4186-4199.

9. A. Pintar, R. Malacea, C. Pinel and M. Besson, *Vib. Spectrosc.*, 2007, **45**, 18-26.